Attenuation of TGF-β signaling suppresses premature senescence in a p21-dependent manner and promotes oncogenic Ras-mediated metastatic transformation in human mammary epithelial cells

Shu Lin[a], Junhua Yang[a], Abdel G. Elkahloun[b], Abhik Bandyopadhyay[a], Long Wang[a], John E. Cornell[c], I-Tien Yeh[d], Joseph Agyin[a], Gail Tomlinson[e], and Lu-Zhe Sun[a,f]

[a]Department of Cellular and Structural Biology, University of Texas Health Science Center, San Antonio, TX 78229; [b]Cancer Genetics Branch, National Human Genome Research Institute, National Institutes of Health, Bethesda, MD 20892; [c]Department of Epidemiology and Biostatistics, [d]Department of Pathology, [e]Greehey Children's Cancer Research Institute, and [f]Cancer Therapy and Research Center, University of Texas Health Science Center, San Antonio, TX 78229

ABSTRACT **The molecular mechanisms that drive triple-negative, basal-like breast cancer progression are elusive. Few molecular targets have been identified for the prevention or treatment of this disease. Here we developed a series of isogenic basal-like human mammary epithelial cells (HMECs) with altered transforming growth factor-β (TGF-β) sensitivity and different malignancy, resembling a full spectrum of basal-like breast carcinogenesis, and determined the molecular mechanisms that contribute to oncogene-induced transformation of basal-like HMECs when TGF-β signaling is attenuated. We found that expression of a dominant-negative type II receptor (DNRII) of TGF-β abrogated autocrine TGF-β signaling in telomerase-immortalized HMECs and suppressed H-Ras-V12–induced senescence-like growth arrest (SLGA). Furthermore, coexpression of DNRII and H-Ras-V12 rendered HMECs highly tumorigenic and metastatic in vivo in comparison with H-Ras-V12–transformed HMECs that spontaneously escaped H-Ras-V12–induced SLGA. Microarray analysis revealed that p21 was the major player mediating Ras-induced SLGA, and attenuated or loss of p21 expression contributed to the escape from SLGA when autocrine TGF-β signaling was blocked in HMECs. Furthermore, knockdown of p21 also suppressed H-Ras-V12–induced SLGA. Our results identify that autocrine TGF-β signaling is an integral part of the cellular anti-transformation network by suppressing the expression of a host of genes, including p21-regulated genes, that mediate oncogene-induced transformation in basal-like breast cancer.**

Monitoring Editor
Kunxin Luo
University of California, Berkeley

Received: Oct 12, 2011
Revised: Feb 13, 2012
Accepted: Feb 17, 2012

This article was published online ahead of print in MBoC in Press (http://www.molbiolcell.org/cgi/doi/10.1091/mbc.E11-10-0849) on February 22, 2012.

Address correspondence to: Lu-Zhe Sun (sunl@uthscsa.edu).

Abbreviations used: DNRII, dominant-negative transforming growth factor-β type II receptor; EGFP, enhanced green fluorescent protein; HMEC, human mammary epithelial cell; hTERT, human telomerase reverse transcriptase; Mit C, mitomycin C; RI, transforming growth factor-β type I receptor; RII, transforming growth factor-β type II receptor; RIKI, RI kinase inhibitor; SA-β-gal, senescence-associated β-galactosidase; SLGA, senescence-like growth arrest; SLP, senescence-like phenotype; TGF-β, transforming growth factor-β.

INTRODUCTION

Breast cancer is the most frequently diagnosed neoplasm in American women and the leading cause of cancer death among nonsmoking females (Jemal *et al*., 2010). Treating malignant breast cancer continues to be a challenge to medical professionals because our knowledge of multifaceted molecular alterations that drive breast carcinogenesis is still quite limited. Gene expression profiling studies revealed that different phenotypes of breast carcinomas could be classified with distinctive gene expression profiles. For example, triple-negative breast carcinomas (estrogen receptor negative [ER–], progesterone receptor negative [PR–], EGFR2/Her2 negative [Her2–]), which often have a poor prognosis, have a basal-like gene expression profile similar to that of human mammary

epithelial cells (HMECs; Perou *et al.*, 2000; Sorlie *et al.*, 2001). However, little is known about the molecular alterations that cause basal-like breast cancer. Unlike ER+ or Her2+ breast carcinomas, there are only few targets for the treatment or prevention of basal-like breast carcinomas, which are highly prevalent in African American women (Carey *et al.*, 2006).

Transforming growth factor-β (TGF-β) signaling is known to suppress epithelial tumorigenesis by inhibiting cell cycle progression, stimulating apoptosis, and promoting genomic stability and cellular senescence (Roberts and Wakefield, 2003). In humans and mice, TGF-β is a homodimeric polypeptide of 25 kDa. Three TGF-β isoforms, termed TGF-β1, β2, and β3, have been identified in mammals. Secreted TGF-β binds to two different cell surface receptors called type I (RI) and type II (RII) receptors. They are serine/threonine kinase receptors, which also contain the tyrosine kinase domain. Binding of TGF-β to RII leads to the recruitment, phosphorylation, and activation of RI. The activated RI phosphorylates intracellular Smad2 and Smad3, which then interact with Smad4 protein to form an oligomeric complex. Once transported into nuclei, the Smad2/Smad3/Smad4 complex binds to specific DNA sequences and they act as transcription activators or repressors, depending on DNA sequence and cellular context (Massague, 2008).

TGF-β signaling components have been shown to be mutated in certain types of carcinomas and attenuated in many others. In human breast cancer, mutational inactivation of TGF-β receptors or its intracellular signal transducers—Smad proteins—is rare (Bierie and Moses, 2006). However, reduced expression of RII has been associated with tumor progression (de Jong *et al.*, 1998; Gobbi *et al.*, 1999). To our knowledge, how the impaired TGF-β receptor signaling alters genome-wide transcription profile resulting in oncogene-induced transformation and malignant progression in HMECs has not been clearly described. On the other hand, blockade of TGF-β signaling with the expression of a transgenic dominant-negative RII (DNRII) or deletion of RII gene only increased cell proliferation, with no evidence of tumorigenesis in mammary gland, pancreas, and epidermis in mice (Bottinger *et al.*, 1997a, 1997b; Wang *et al.*, 1997), suggesting that the attenuation of TGF-β signaling alone appears insufficient for transformation.

Oncogenes, such as H-Ras-V12, are known to induce premature senescence in murine fibroblasts and HMECs in vitro by activating p16ink4a/Rb and p53 pathways (Serrano *et al.*, 1997). More recently, several studies have reported senescence-like phenotypes (SLPs) in early stages of neoplasm in various human and mouse tissues, including breast tumors (Bartkova *et al.*, 2005; Braig *et al.*, 2005; Chen *et al.*, 2005; Collado *et al.*, 2005; Michaloglou *et al.*, 2005). However, many breast cancer cells and tissues show gene signature expression profiles resembling Ras activation (Bild *et al.*, 2006). In addition, oncogenic Ras has been shown to cooperate with mutant p53 to switch TGF-β to be a tumor promoter in enhancing the progression of breast cancer (Adorno *et al.*, 2009). Thus, bypassing oncogene-induced SLP appears to be a limiting step for tumorigenesis. Significantly, attenuation of TGF-β signaling in mouse keratinocytes was shown to overcome H-Ras-V12–induced premature senescence (Tremain *et al.*, 2000). However, the biology of mouse keratinocytes may not be the same as that of HMECs, and how attenuation of TGF-β signaling can suppress SLP and facilitate malignant transformation by an oncogene in HMECs has not been studied. Given that HMEC resembles basal-like estrogen receptor–negative breast cancer and is an appropriate model for the study of basal-like breast cancer, we used it to elucidate how the attenuation of autocrine TGF-β signaling serves as a key step in leading to oncogenic transformation and metastatic progression upon

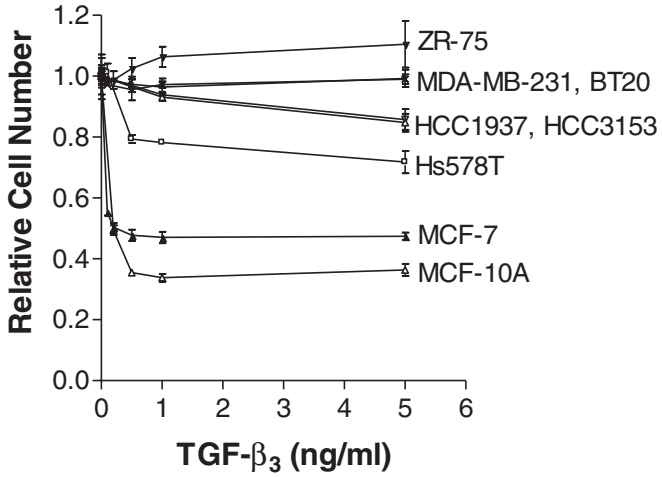

FIGURE 1: TGF-β signaling is attenuated in human triple-negative breast cancer cell lines. Breast cancer cells were plated in 96-well plates at 2000 cells/well and treated with various concentrations of TGF-β3 as depicted. MTT assays were performed after 5 d to obtain relative cell numbers. Each point is the mean ± SEM of four replicate wells.

expression of the human telomerase reverse transcriptase (hTERT) and H-Ras-V12.

We generated a series of isogenic HMECs representing a full spectrum of basal-like breast carcinogenesis to identify candidate genes that mediate the escape of oncogene-induced senescence and malignant transformation of basal-like breast cancer. We found that autocrine TGF-β signaling is an integral part of cellular anti-transformation network by suppressing the expression of a host of genes, including p21-regulated genes that mediate oncogene-induced transformation. Our study shows that abrogation of autocrine TGF-β signaling can promote malignant progression of H-Ras-V12–transformed HMECs in both in vitro and in vivo settings. Our novel finding modifies the current dogma that TGF-β inhibits breast carcinogenesis by simply inhibiting cell proliferation and provides novel insights into the mechanism of the cross-talk between the TGF-β signaling and oncogenic Ras signaling in basal-like breast cancer development and progression.

RESULTS

TGF-β signaling is attenuated in human triple-negative breast cancer cell lines

Reduced expression of RII and Smad4 in human breast tissues has been associated with breast tumorigenesis and progression (de Jong *et al.*, 1998; Gobbi *et al.*, 1999; Stuelten *et al.*, 2006). Many breast cancer cell lines are also known to express low levels of RII (Pouliot and Labrie, 1999; Lynch *et al.*, 2001). As a result, they are often resistant to the growth-inhibitory activity of TGF-β. We found that, in contrast to the untransformed MCF-10A mammary epithelial cells, many triple-negative human breast cancer cell lines, including MDA-MB-231, BT20, Hs578T, HCC1937, and HCC3153, are resistant to the growth-inhibitory activity of TGF-β (Figure 1). Thus the attenuation of TGF-β signaling is likely a hallmark of breast tumorigenesis in some triple-negative breast cancer patients.

Generation of hTERT-immortalized HMEC/DNRII cells

Because HMECs from primary cultures are considered appropriate models for studying triple-negative basal-like breast cancer (Ross and Perou, 2001; Troester *et al.*, 2004), we immortalized HMECs

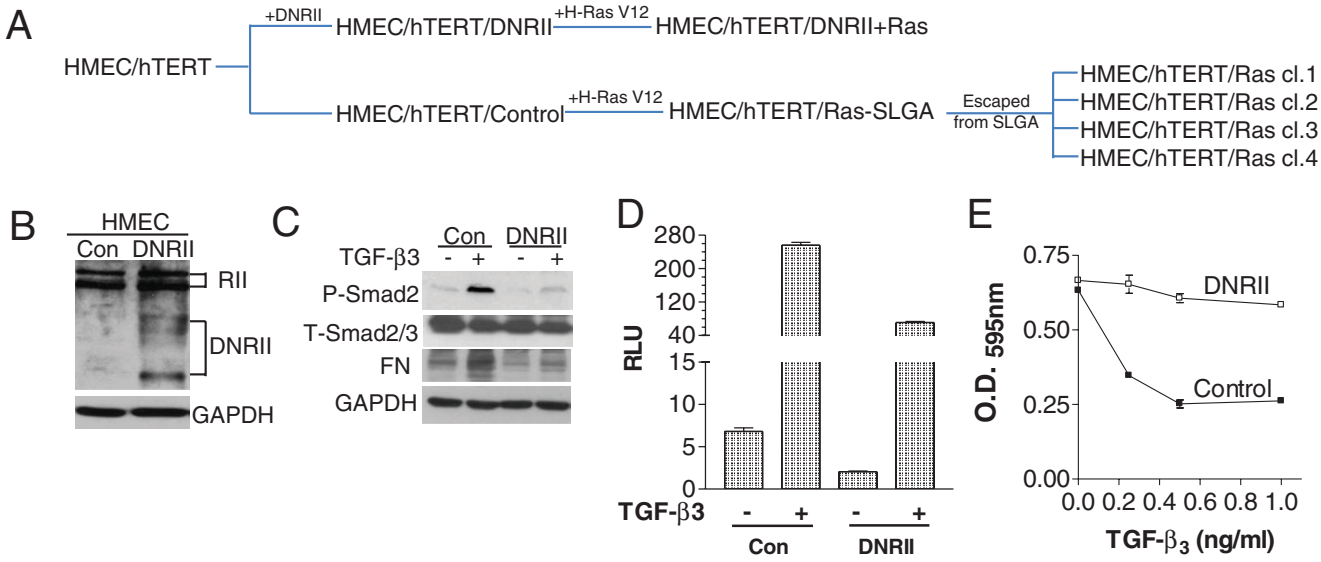

FIGURE 2: Generation of hTERT-immortalized HMEC/DNRII cells. (A) A schematic flowchart of generating the hTERT-immortalized HMEC cell lines with altered TGF-β sensitivity, ectopic H-Ras-V12 expression, and different phenotypes. (B) DNRII protein expression was detectable in the DNRII and control (Con) HMECs with a Western blotting analysis. Glyceraldehyde-3-phosphate dehydrogenase (GAPDH) level was used to validate equal sample loading. (C) Control and DNRII HMECs were treated with or without 80 pM (2 ng/ml) TGF-β3 for 16 h, and cell lysate was used for Western blotting to detect phosphorylated Smad2 (P-Smad2), total Smad2/3 (T-Smad2/3), fibronectin (FN), and other gene products as depicted. (D) Control and DNRII HMECs were transiently transfected with pSBE4-Luc and β-gal expression constructs. Cells were treated with or without TGF-β3 (2 ng/ml) for 17 h. β-Gal–normalized luciferase activity (RLU) is presented as mean ± SEM from three transfections. (E) Control and DNRII HMECs were seeded in a 96-well plate at 2000 cells/well for 2 h and treated with indicated different concentrations of TGF-β3 for 4 d. MTT assay was performed to obtain OD values reflecting relative cell number. Each data point represents the mean ± SEM from four wells.

with the hTERT as previously done by others (Elenbaas *et al.*, 2001) and used the immortalized HMECs to determine the role of autocrine TGF-β signaling in breast carcinogenesis. To mimic the attenuated TGF-β signaling in breast cancer cell lines and tissues, we stably introduced a dominant-negative TGF-β RII (DNRII) into the immortalized HMECs as shown in Figure 2, A and B. Control cells were transfected with an empty vector. The expression of DNRII significantly attenuated TGF-β receptor signal transduction as reflected by a reduction of basal phosphorylated Smad2 (P-Smad2) and fibronectin (FN) and a more pronounced reduction of TGF-β–stimulated P-Smad2 and FN levels in the DNRII cells (Figure 2C). DNRII expression also significantly reduced basal as well as TGF-β–stimulated Smad-responsive promoter activity, as shown in Figure 2C. Because HMECs were cultured in a serum-free (consequently TGF-β–free) medium, the change of basal gene expression and promoter activity due to DNRII expression indicated that DNRII attenuated autocrine TGF-β signaling. Although DNRII expression only partially blocked TGF-β-induced P-Smad2 and TGF-β–responsive promoter activity (Figure 2, C and D), DNRII cells were resistant to the growth inhibitory activity of TGF-β, as shown in Figure 2E. Thus DNRII cells show similar TGF-β responsive properties shared by triple-negative breast cancer cells, as shown in Figure 1.

Blockade of TGF-β signaling inhibits H-Ras-V12–induced SLGA in HMECs

Because many breast cancer cells exhibit enhanced signature pathways resembling Ras activation (Bild *et al.*, 2006), we transfected HMEC control and DNRII cells with the oncogenic H-Ras-V12 in an attempt to generate transformed cell lines. Of interest, expression of H-Ras-V12 in the control cells induced senescence-like phenotypes (SLPs) such as the expression of senescence-associated β-galactosidase (SA-β-gal; Dimri *et al.*, 1995; Figure 3A), enlarged cell shape, and cessation of cell proliferation, with a reduced level of phosphorylated Rb (P-Rb) protein in comparison with DNRII + Ras cell (Figure 3B). Similar to the effect of DNRII, treatment of the control HMECs with an RI kinase inhibitor (RIKI, LY-364947) also prevented Ras-induced SLP, whereas removal of RIKI after Ras expression restored SLP (Figure 3C). Although HMECs, like many breast cancer cell lines, do not express a detectable level of p16ink4a due to methylation-mediated silencing of its promoter (Rocco and Sidransky, 2001), and increased expression of p16ink4a is believed to be necessary for the maintenance of H-Ras-V12-induced senescence in normal human fibroblasts (Serrano *et al.*, 1997), we found that the H-Ras-V12–induced senescence-like phenotypes were quite stable since only a few cells out of thousands of growth-arrested cells occasionally escaped from the arrest after several weeks of culture. However, to distinguish p16ink4a-mediated senescence from the senescence-like phenotypes in HMEC/Ras cells, we use the term senescence-like growth arrest (SLGA) for the latter.

H-Ras-V12 HMEC clones spontaneously escape from SLGA without increasing active autocrine TGF-β

To obtain HMECs spontaneously recovered from H-Ras-V12–induced SLGA, we plated senescence-like HMEC Ras cells in soft agarose and isolated a few colonies. These Ras clones were found to be transformed, since they could form colonies when replated in soft agarose (unpublished data). They retained high expression of the transfected Ras when compared with growth-arrested control + Ras cells (called Ras-SLGA hereafter) and DNRII + Ras cells, as shown for one of the Ras clones, called Ras cl.4 hereafter, in Figure 4A. Ras cl.4

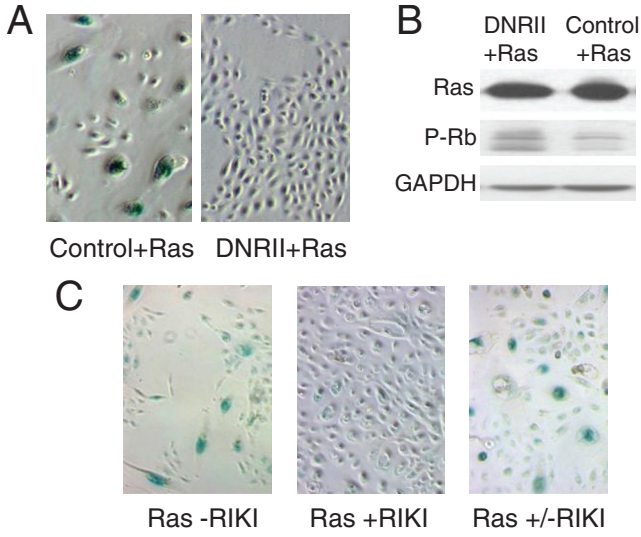

FIGURE 3: Blockade of TGF-β signaling inhibits Ras-induced senescence-like phenotypes. (A) Control and DNRII HMECs were transduced with a retrovirus carrying an expression cassette of H-Ras-V12. The stable cells were stained for SA-β-gal activity when the H-Ras-V12 cells showed senescence-like morphology. Elevated SA-β-gal activity was detected in the cells transfected with H-Ras-V12 as indicated with the dark, bluish-green staining. (B) Lysate of the DNRII + Ras and control + Ras cells were used in Western blotting for the measurements of the levels of total Ras (Pan-Ras), phosphorylated Rb (P-Rb), and GAPDH. (C) HMECs were treated without (–RIKI) or with (+RIKI) TβRI kinase inhibitor at 100 nM for 1 d and then transduced with Ras retrovirus. The cells labeled with Ras ± RIKI were initially treated with RIKI during first 8 d of Ras expression and then cultured without RIKI for additional 7 d. All cells were stained for SA-β-gal 15 d after Ras expression, and senescent cells were stained with a dark, bluish-green color as shown in A.

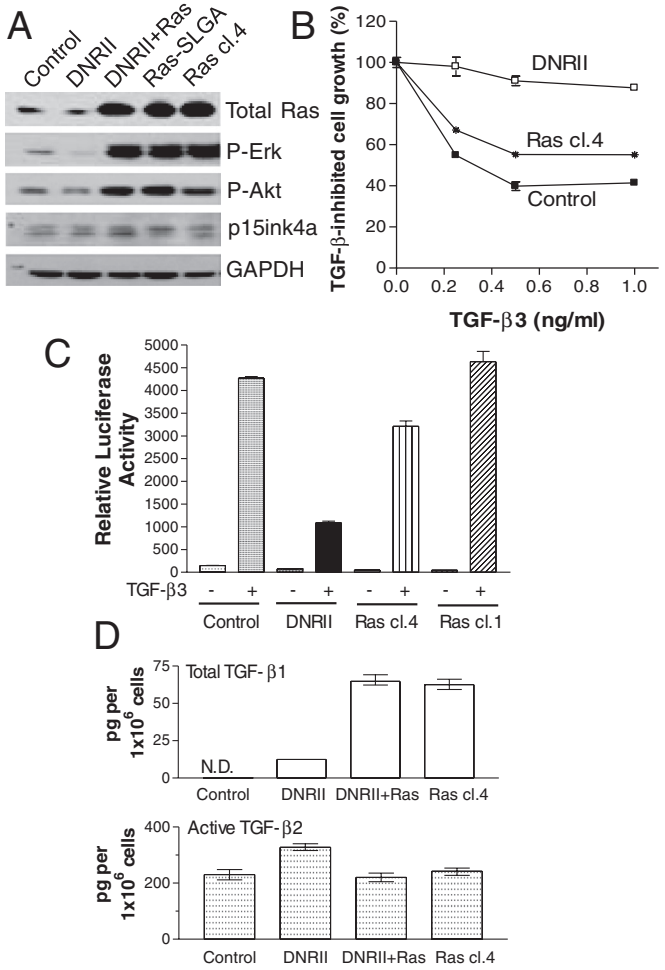

FIGURE 4: H-Ras-V12 HMEC clones spontaneously escape from SLGA. (A) Western analyses of total Ras, phosphorylated Erk (P-Erk), phosphorylated Akt (P-Akt), p15ink4b, and GAPDH in the depicted HMEC lines illustrating that DNRII + Ras, Ras-SLGA, and Ras clone 4 (Ras cl.4) have similar expression levels of these proteins. (B) Cells were plated in 96-well plates at 2000 cells/well and treated with various concentrations of TGF-β3 as depicted. MTT assays were performed after 4 d to obtain relative cell numbers. Each point is the mean ± SEM of four replicate wells. (C) Cells were transfected with pSBE4-Luc and a β-gal expression plasmid. They were then treated with or without TGF-β3 at 2 ng/ml for 19 h. The β-gal activity–normalized relative luciferase activity is shown as mean ± SEM from three transfections. (D) The media conditioned by confluent cultures of the cells in 2 ml for 48 h were used for the measurements of total or active TGF-β1 and TGF-β2 with sELISA.

also contained the active H-Ras-V12, since it expressed increased levels of the phosphorylated Erk and Akt, similar to those in DNRII + Ras and Ras-SLGA (Figure 4A). Of interest, Ras cl.4 was less sensitive to the growth-inhibitory activity of TGF-β than the control HMECs, suggesting dysregulation of TGF-β growth-inhibitory pathway by the oncogenic Ras (Figure 4B). However, Ras cl.4 and Ras cl.1, one of other Ras clones that escaped from H-Ras-V12–induced SLGA, were fully responsive to the transcriptional activity of TGF-β (Figure 4C). Previous study showed that H-Ras-V12 expression drastically increased total and active TGF-β1 secretion into the medium conditioned by mouse keratinocytes (Tremain *et al.*, 2000), which should significantly increase autocrine TGF-β activity. We found, in fact, that the total TGF-β1 level in the medium conditioned by the control cells was below the detection limit of 15 pg/ml (Figure 4D, N.D.). Although H-Ras-V12 expression significantly increased total TGF-β1 in the conditioned media of DNRII + Ras and Ras cl.4 cells (Figure 4D), this level was still considerably (~10 times) lower than what was reported for the Ras-transfected mouse keratinocytes. In addition, the active form of TGF-β1 in the media conditioned by Ras-transfected HMECs was undetectable. On the other hand, HMECs produced readily detectable levels of active TGF-β2. However, neither the total TGF-β2 (unpublished data) nor the active TGF-β2 was increased by H-Ras-V12 expression (Figure 4D). This indicates that H-Ras-V12 expression does not increase the autocrine TGF-β activity in the HMECs. It should be noted that we have previously showed that the triple-negative breast cancer MDA-MB-231 cells also produce significantly higher TGF-β2 than TGF-β1 (Bandyopadhyay *et al.*, 1999).

Blockage of TGF-β signaling enhances oncogenic Ras-induced tumorigenesis and metastasis

Because the abrogation of autocrine TGF-β signaling with DNRII expression overcame H-Ras-V12–induced SLGA, we next compared the tumorigenicity and metastatic potential of DNRII + Ras cells with Ras clones in female nude mice. We found orthotopic injection of the enhanced green fluorescent protein (EGFP)–labeled DNRII + Ras cells mixed with Matrigel produced larger orthotopic tumors than EGFP-labeled Ras clones mixed with Matrigel with 100% incidence (Figure 5, A and B). By using green fluorescence imaging to detect micrometastases in excised lungs, we found that all mice inoculated with DNRII + Ras cells had more and larger lung metastasis colonies than the mice inoculated with Ras cl.1 (Figure 5C). Because

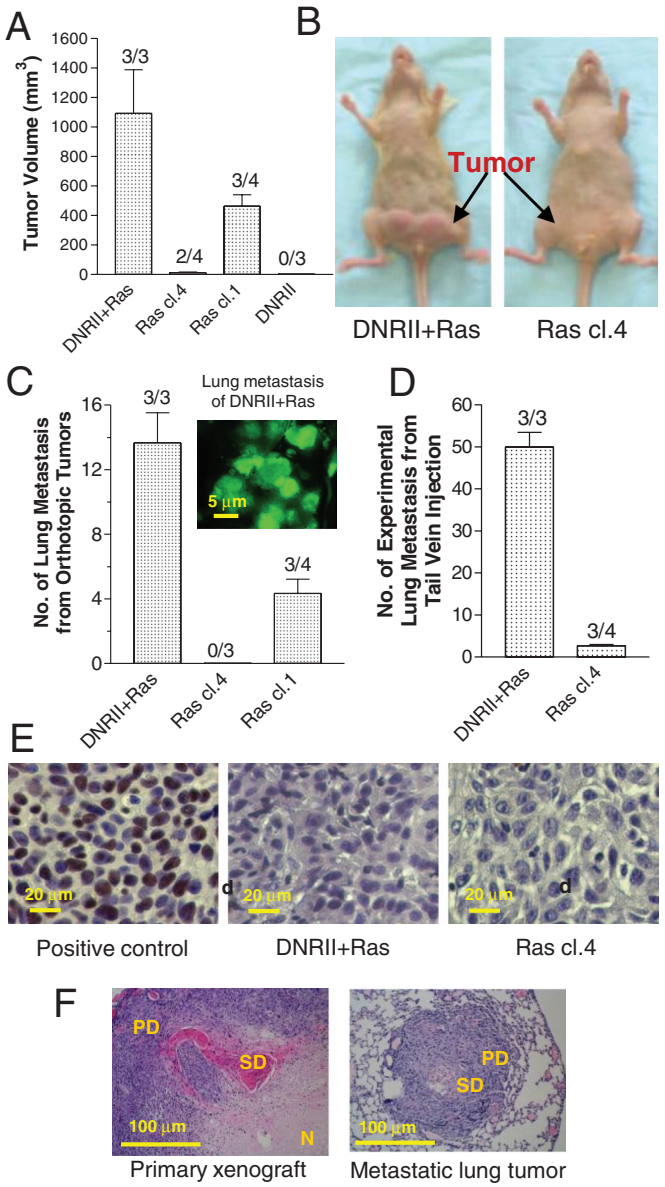

FIGURE 5: Tumorigenic and metastatic properties of HMEC Ras clones and DNRII + Ras. (A) EGFP-labeled cells were injected orthotopically into both inguinal mammary glands using 4×10^6 cells/site for DNRII + Ras and 10×10^6 cells/site for all other cells. The suspended cells were mixed with Matrigel at 1:1 ratio before injection. Four weeks after injection, tumor volumes were obtained with a caliper using the equation $V = (L \times W^2) \times 0.5$, where V is volume, L is length, and W is width. The data are presented as mean ± SEM from four to six tumors in two or three mice. The numbers on each column indicate tumor incidence in the inoculated mice. (B) Representative orthotopic tumors of DNRII + Ras– and Ras cl.4–inoculated mice. (C) Green metastatic lung colonies in the lungs of the mice described in A were counted under an inverted fluorescence microscope. The data are presented as mean ± SEM from three mice. The numbers on each column indicate spontaneous metastasis incidence in the inoculated mice. A representative green fluorescence image (×40 magnification) was taken from a lung of a mouse inoculated with DNRII + Ras cells. (D) Number of lung metastases in mice injected with 0.2×10^6 DNRII + Ras or Ras cl.4 cells through the tail vein. Green fluorescent lung metastases were counted after 10 wk and presented as mean ± SEM from three mice. (E) Histological examination for human ER-α expression of the primary tumors formed by DNRII + Ras or Ras cl.4 cells. ER-α–positive ZR-75-1 xenograft was used as a positive control. (F) Histological examination of the primary tumors and lung metastases formed by DNRII + Ras cells revealed poorly differentiated areas (PD) that are spindled and epithelioid. Some areas showed squamous differentiation with keratin pearl formation (SD). Some necrotic areas in the primary tumor (N) were also observed.

orthotopically inoculated Ras cl.4 formed very small tumors and thus did not metastasize to lung (Figure 5C), we also injected DNRII + Ras and Ras cl.4 cells in the tail vein to compare their metastatic potential. Although the mice injected with Ras cl.4 showed some lung metastasis colonies, those injected with DNRII + Ras had many more lung metastasis colonies (Figure 5D). As such, while Ras clones are transformed, they are much less malignant than DNRII + Ras cells, thus representing early neoplastic cells. On the other hand, the DNRII + Ras cell–formed tumors showed similar features as basal-like breast cancer, such as a high frequency of visceral metastasis. To further demonstrate that our models derived from HMEC cells indeed reflected the triple-negative breast cancer process, we confirmed that the tumors derived from Ras cl.4 and DNRII + Ras cells were ER-negative (Figure 5E). We also found that some DNRII + Ras cell–formed tumors contained necrotic foci and squamous metaplasia (Figure 5F) and did not metastasize to bone even when the cells were inoculated in the arterial circulation (unpublished data). These are also the reported features of basal-like breast cancer (Livasy *et al.*, 2006; Rodriguez-Pinilla *et al.*, 2006). Thus the metastatic potential of DNRII + Ras cells appears to correlate with that of late-stage basal-like breast cancer cells.

Genome-wide transcript profiles of a series of isogenic basal-like HMEC lines

To find the gene signature that contributes to SLGA by H-Ras-V12, the escape from SLGA, tumorigenesis, and metastasis, we performed gene expression microarray using Affymetrix HG-U133_Plus_2 chips containing 54,743 probes for the human genome. Of interest, many previously identified genes related to breast cancer metastasis, poor prognosis, and basal-like markers in clinical samples (van't Veer *et al.*, 2002; Minn *et al.*, 2005; Wang *et al.*, 2005) were found to be highly up-regulated in DNRII + Ras cells when compared with the control cell (Supplemental Table S1), again demonstrating the clinical relevance of our model systems. Because of the multiple cell lines with different properties in senescence and malignancy used in our gene expression profiling, we were able to perform combinatorial/clustering analyses across various comparisons. For example, by asking what genes are up-regulated in the cells that escaped SLGA and are also up-regulated by the blockade of autocrine TGF-β signaling, we pulled out the genes that are up-regulated in Ras cl.4 versus Ras-SLGA, DNRII + Ras versus Ras-SLGA, and DNRII versus control. Of interest, many genes that are involved in the regulation of mitosis and G2/M cell cycle checkpoints were among the most highly increased genes, as listed in Table 1. The changes of AURKB, CDC2, and STK6/AURA transcripts in Table 1 were confirmed with real time (RT)-PCR (Supplemental Figure S1).

Abrogation of autocrine TGF-β overcame H-Ras-V12–induced SLGA with a significant reduction of p21 level and transcriptional activity of p53

One gene worth noting from our microarray data is p21. p21 is known to be stimulated by TGF-β in a p53-independent manner (Datto *et al.*, 1995), and its transcript was down-regulated by 30% in DNRII cells in comparison with the control according to our microarray

Gene symbol	Gene title annotation	Fold changes		
		DNRII/control	Ras cl.4/Ras-SLGA	DNRII + Ras/Ras-SLGA
ASPM	asp (abnormal spindle)-like	10.71553	23.765926	17.058058
AURKB	Aurora kinase B	4.652449	12.334759	13.678273
BUB1	Spindle check point kinase	9.308313	21.99638	19.951128
BUB1B	Spindle check point kinase	9.627348	18.713463	16.873495
CCNA2	Cyclin A2	5.4355903	16.283352	13.300644
CCNB2	Cyclin B2	6.9319105	11.787509	9.785267
CDC2/CDK1	Cell division cycle 2, G1 to S and G2 to M	13.984082	49.193413	46.213715
CDCA1	Cell division cycle associated 1	12.695456	28.146688	27.312359
CENPA	Centromere protein A, 17 kDa	9.051207	22.97814	22.432482
DLG7/HURP	Discs, large homologue 7 (*Drosophila*)	10.798248	34.466877	31.79402
GTSE1	G2 and S-phase expressed 1	4.165664	9.154935	12.93397
HCAP-G	Chromosome condensation protein G	19.232702	41.89133	45.201603
KIF14	Kinesin family member 14	5.7058287	13.420322	11.990353
KIF18A	Kinesin family member 18A	5.2050924	10.034681	9.987414
KIF20A	Kinesin family member 20A	8.074748	16.617043	16.89858
KIF23	Kinesin family member 23	5.9767056	13.2807045	16.004639
KIF2C	Kinesin family member 2C	8.064909	18.539717	16.51991
KIF4A	Kinesin family member 4A	5.618885	12.100409	9.718895
KNTC2	Kinetochore associated 2	19.95345	40.17909	40.846714
NEK2	(Never in mitosis gene a)-related kinase 2	10.480386	26.178247	22.477205
SPBC25	Spindle pole body component 25 homologue	8.240608	12.467526	16.724138
STK6/AURA	Serine/threonine kinase 6, Aurora A	8.10627	13.344038	15.343063
TTK	TTK protein kinase	11.721804	28.365597	23.66676
UBE2C	Ubiquitin-conjugating enzyme E2C	8.90135	18.48864	17.525461
ZWINT	ZW10 interactor	8.879728	30.042128	29.499672

TABLE 1: Suppressors of SLGA that are inhibited by autocrine TGF-β signaling.

analysis (Figure 6A). Of interest, it was more significantly down-regulated in DNRII + Ras and Ras cl.4 cells. The down-regulation of p21 transcript also resulted in decreased p21 protein levels, as shown with the Western blotting (Figure 6B). In fact, p21 protein was undetectable in both Ras cl.4 and Ras cl.1, and its levels were not correlated with p53 levels (Figure 6B). Similar to the effect of DNRII, treatment of HMECs with the RIKI also reduced p21 protein level by 48% (Figure 6C) and led to the suppression of Ras-induced SLGA (Figure 3D).

In addition to Ras cl.4 and Ras cl.1, we also screened two additional Ras clones that escaped from H-Ras-V12–induced SLGA for their expression of p53 and p21. Treatment of the cells with the DNA-damaging agent mitomycin C (Mit C) induced p53 expression in all cells except Ras cl.3 (Figure 6D). Ras cl.3 has a high basal level of p53, suggesting that it may have a mutated p53. Whereas p53 was up-regulated by Mit C in other Ras clones, p21 was not detectable in Ras cl.4 and Ras cl.1 as expected, and was not regulated by p53 in Ras cl.2. Of interest, p21 could still be stimulated by TGF-β in Ras cl.2, as shown in Figure 6E. Thus the escape from H-Ras-V12-induced SLGA is associated with loss of p21 regulation by p53 in these Ras clones. On the other hand, abrogation of autocrine TGF-β overcame H-Ras-V12–induced SLGA, with a significant reduction of p21 level (Figure 6A) and apparent attenuation of p53-induced p21 expression in DNRII + Ras cells, as shown in Figure 6D.

Because the ability of Mit C–induced p53 to increase p21 expression is attenuated in DNRII HMECs in comparison to the control (Figure 6D), we further determined whether p53 activity was decreased by the abrogation of autocrine TGF-β signaling in DNRII HMECs. We transiently cotransfected a β-gal expression plasmid with a p53-responsive p21 promoter-luciferase or a PCNA promoter-luciferase reporter into the control and DNRII HMECs. The cells were then treated with Mit C to induce DNA damage and p53 expression. Treatment with Mit C increased a similar level of p53 in the control, DNRII, and DNRII + Ras cells, as shown in Figure 6D. It significantly stimulated the luciferase activity in the control cells. However, the stimulation was attenuated in DNRII cells for both promoters (Figure 6F). Site-directed mutation of the p53-responsive element in the PCNA promoter abolished the effect of Mit C treatment (unpublished data), suggesting that the Mit C–induced promoter activity was due to increased transcriptional activity of p53. Next we performed chromatin immunoprecipitation (ChIP) assays coupled with quantitative PCR (qPCR) to determine whether the amount of p53 bound to p53-responsive promoters was inhibited by the abrogation of autocrine TGF-β signaling among the control, DNRII,

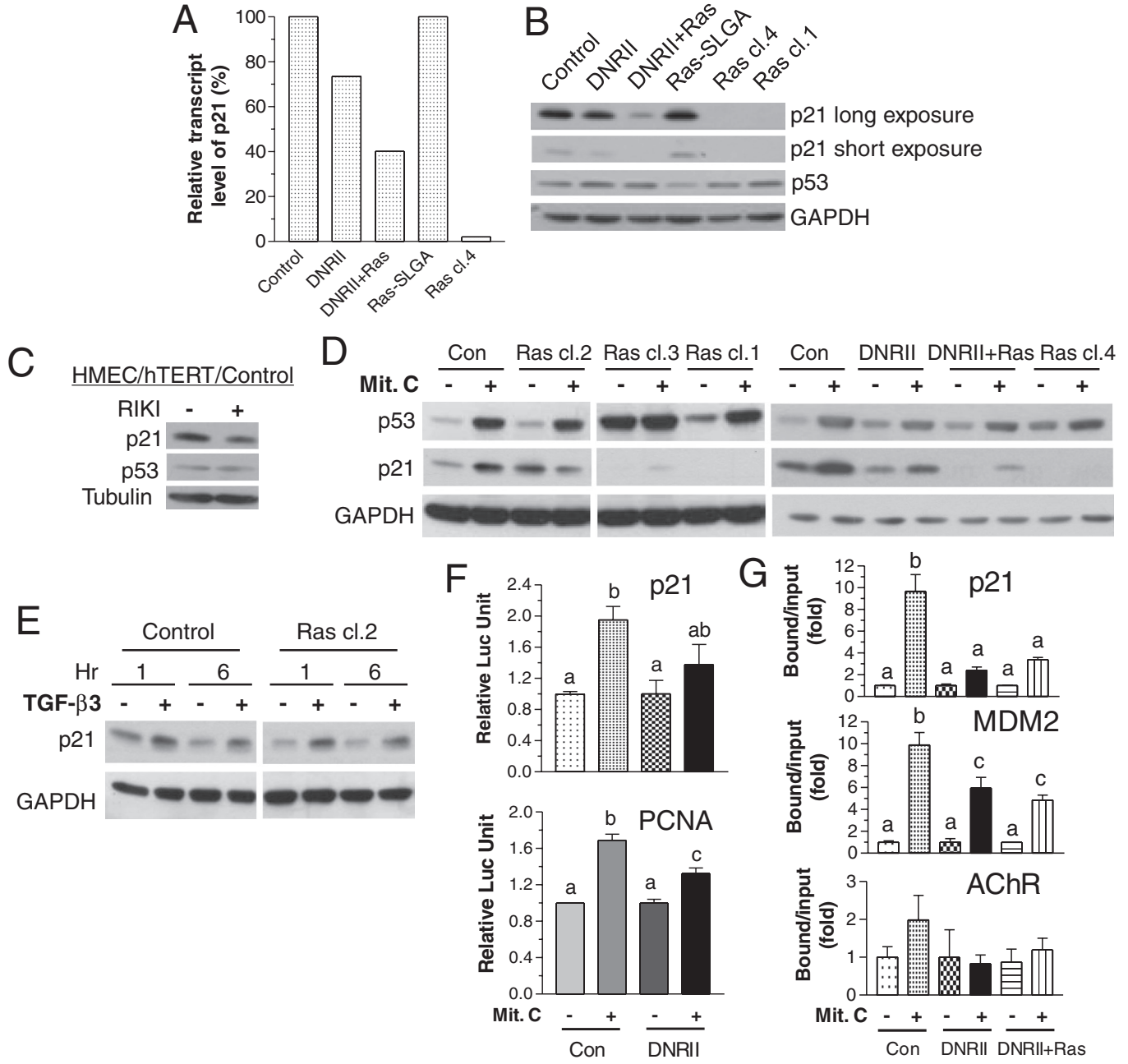

FIGURE 6: Blockade of TGF-β signaling overcomes H-Ras-V12–induced SLGA with significant down-regulation of p21 and transcriptional activity of p53. (A) p21 transcript levels in various HMEC cells normalized to that of the control cells from the microarray analysis. (B) p21, p53, and GAPDH protein levels in the cells analyzed with Western blotting. (C) HMEC control cells were treated without (Con) or with 100 nM RIKI for 4 d. p21 and p53 levels in the cells were measured with Western blotting. (D) Various HMEC cells were treated with Mit C at 5 μg/ml for 22 h. The cells were then harvested, and their extracts were used in Western blotting to measure the levels of p53, p21, and GAPDH. (E) Control and Ras cl.2 were treated with TGF-β3 at 1 ng/ml for depicted time. Cell extracts were used in Western blotting to measure the levels of p21. (F) Control (Con) and DNRII HMECs were transiently cotransfected with a β-gal expression plasmid and a p53-responsive p21 promoter-luciferase (Luc) or PCNA promoter-Luc plasmid. The transfected cells were then treated without or with Mit C at 5 μg/ml for 21 h. Luciferase activity was normalized with β-gal activity, and the relative luciferase activity of each cell line without Mit C treatment was converted to one unit to allow statistical comparison across all groups. (G) Control, DNRII, and DNRII + Ras cells were treated without or with Mit C as in F. The chromatin was cross-linked and immunoprecipitated with a p53 antibody as described in *Materials and Methods*. The amount of p53 binding sequences in p21 and MDM2 promoters in the input control and precipitated with the anti-p53 antibody was measured with qPCR. AChR promoter was used as a negative control. The percentage total promoter occupancy of each cell line without Mit C treatment was converted to one unit for statistical comparison across all groups. Each value is the mean ± SEM from three transfections for F or three qPCR for E. The bars bearing a different letter are significantly different at $p < 0.05$ detected with one-way ANOVA.

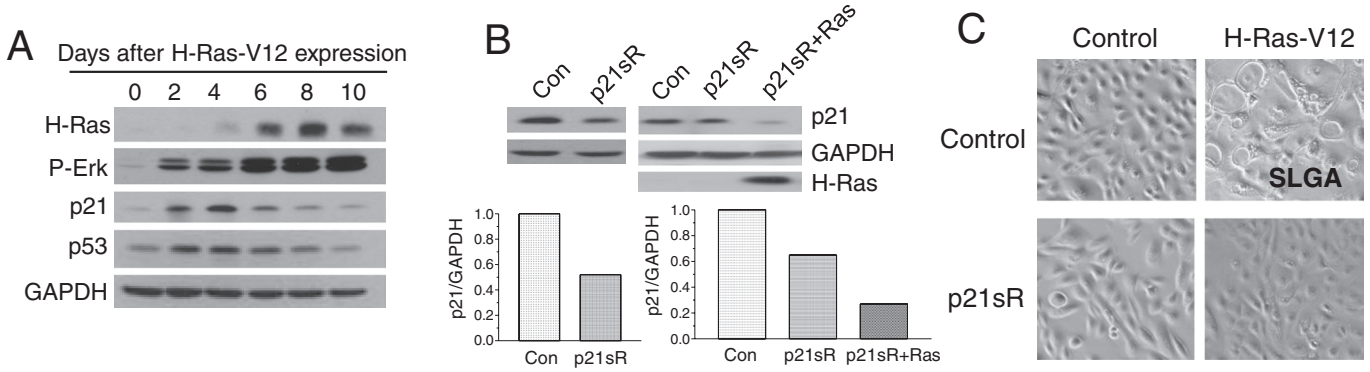

FIGURE 7: A high level of p21 expression is necessary for H-Ras-V12–induced SLGA. (A) HMECs were infected with H-Ras-V12–containing retrovirus. After depicted days of Ras expression, the cells were harvested for Western blotting analysis of indicated gene expression. The cells exhibited SLGA after 6–8 d of Ras expression. (B) HMECs were infected with retrovirus containing a control (Con) or a p21 shRNA (p21sR). The stably infected cells were then infected with the H-Ras-V12–containing retrovirus. Western blotting analyses were performed to detect p21 expression in these cells. The bar figures under the Western blots are GAPDH-normalized p21 levels quantified with Image-Pro software (Media Cybernetics, Bethesda, MD). (C) Representative images of HMECs infected with control, p21 shRNA, and/or H-Ras-V12 retroviruses (100× magnification). The control cells expressing H-Ras-V12 were growth arrested and showed an enlarged, flattened senescent morphology, whereas p21 shRNA cells proliferated like control cells after H-Ras-V12 expression.

and DNRII + Ras HMECs. As shown in Figure 6G, the treatment with Mit C significantly stimulated the occupancy of p53 at the two p53-responsive promoters of p21 and MDM2 but not at the negative control promoter of acetylcholine receptor (AChR) in the control cells. In contrast, p53 occupancy at p21 and MDM2 promoters was significantly attenuated in the DNRII and DNRII + Ras cells. These data, together with the data shown in Figure 6D, indicate that p53 activity is partially inhibited by the blockade of TGF-β signaling.

A high level of p21 expression is necessary for H-Ras-V12–induced SLGA

p21 is known to be transiently stimulated in a p53-dependent manner during DNA damage response or the induction of premature senescence by H-Ras-V12 in fibroblasts and is believed to be responsible for the initial cell cycle arrest (Serrano *et al.*, 1997; Roninson, 2002). We also observed the transient changes of p53 and p21 when H-Ras-V12 was expressed in HMECs (Figure 7A). Of interest, both p53 and p21 levels started to rise 2 d after the infection by H-Ras-V12 retrovirus, when H-Ras level was not noticeably increased. This could be due to our inability to detect a subtle H-Ras increase at day 2, since phosphorylated Erk proteins were significantly increased due to H-Ras-V12 transfection (Figure 7A). A significant increase of H-Ras-V12 expression was observed on days 6 and 8, when the cells started to exhibit SLGA and p21 levels started to return to the level of the control cell (as at day 0).

Published studies have shown that deletion of p21 gene is not sufficient for mouse fibroblasts to bypass Ras-induced senescence (Pantoja and Serrano, 1999) but is sufficient for the transformation of mouse keratinocytes by Ras (Missero *et al.*, 1996). Because abrogation of TGF-β signaling with DNRII expression or RIKI treatment resulted in a modest reduction (30–50%) of p21 (Figure 6), induction of many p21-inhibited genes (Table 1), and suppression of H-Ras-V12–induced SLGA (Figure 3), we hypothesized that a modest reduction of p21 may be sufficient to alter the expression of many genes and consequently suppress H-Ras-V12–induced SLGA in HMECs. Therefore we stably infected HMECs with a p21 short hairpin RNA (shRNA)–expressing retrovirus, which resulted in a modest (35–50%) reduction of endogenous p21 level (Figure 7B). Of interest, the expression of H-Ras-V12 in the p21 shRNA–expressing cells did not induce SLGA, whereas it did induce SLGA in the control cells, as expected (Figure 7C). Thus our data demonstrate that a modest down-regulation of p21 is sufficient for the escape of Ras-induced SLGA, suggesting that p21 is a major mediator for the regulation of Ras-induced SLGA by autocrine TGF-β signaling.

DISCUSSION

Triple-negative, basal-like breast cancer is highly aggressive and has a poor prognosis. The molecular mechanisms that drive its progression are not well understood, and few molecular targets have been identified for its prevention or treatment. Our study demonstrates that triple-negative human breast cancer cell lines show attenuated TGF-β signaling. Therefore we generated a series of isogenic HMECs with altered TGF-β sensitivity and different malignancy, representing a full spectrum of basal-like breast carcinogenesis. To identify candidate genes that may mediate the escape of H-Ras-V12–induced premature senescence and the oncogene-induced transformation of the basal-like HMECs when TGF-β signaling is attenuated, we determined gene expression profiles of five HMEC lines: control, DNRII, DNRII + H-Ras-V12 (named DNRII + Ras, which was spontaneously metastatic), H-Ras-V12 pool (named Ras-SLGA, which was senescent), and an H-Ras-V12 clone (named Ras cl.4, which escaped from SLGA and was weakly tumorigenic). Our study indeed identifies the molecular pathways and networks involved in the development and progression of the basal-like breast cancer, as well as the potential utility of targeting TGF-β pathway for the inhibition of metastasis induced by triple-negative basal-like breast cancer cells.

In our study, we found that abrogation of autocrine TGF-β signaling with the expression of a DNRII or the use of RIKI in telomerase-immortalized HMECs suppressed H-Ras-V12–induced SLGA. TGF-β–mediated regulation of oncogene-induced premature senescence likely involves multiple pathways, which may depend on cellular context. For example, in mouse keratinocytes, oncogenic Ras expression significantly induced the production of active TGF-β1, which led to the inhibition of c-Myc and the stimulation of p15ink4b, resulting in senescence. Of interest, p21 was not regulated by exogenous and

autocrine TGF-β in the mouse keratinocytes (Tremain *et al.*, 2000; Vijayachandra *et al.*, 2003). In contrast, the HMECs we used produce very little total TGF-β1 and do not produce a detectable level of active TGF-β1 even after Ras expression. After we found that the expression of DNRII or the use of RIKI could suppress Ras-induced senescence in HMECs, we performed an extensive gene microarray in five isogenic HMEC lines and Western blots to search for the alteration of cell cycle regulatory genes and TGF-β target genes such as p21, p15, and c-Myc that may be responsible for DNRII-induced escape from senescence. p21 was found to be moderately reduced in DNRII HMECs and dysregulated in various Ras-expressing clones, but not p15 and c-Myc. To address whether a moderate reduction of p21 in DNRII HMECs was sufficient to suppress Ras-induced SLGA, we knocked down p21, which showed that a moderate reduction of p21 was sufficient to evade Ras-induced SLGA. Thus our results indicate that, whereas TGF-β signaling is necessary for the induction of SLGA by Ras in both mouse keratinocytes and HMECs, the molecular pathways that mediate TGF-β–regulated SLGA are very different between the two cells.

Recently it was shown that the Smad4 inactivation in mouse prostate epithelium with Pten loss can bypass the oncogene-induced senescence (OIS) and enhance tumor cell proliferation and metastasis when compared with the mouse prostate with only Pten loss, indicating that TGF-β/Smad4 signaling as a barrier can inhibit prostate cancer progressing from intraepithelial neoplasia to highly metastatic adenocarcinoma (Ding *et al.*, 2011). In addition, it was reported that TGF-β–inhibited miR-200 has a biphasic role in mediating the epithelial-to-mesenchymal transition and mesenchymal-to-epithelial transition during different stages of metastasis. In particular, elevated miR-200 expression is required to efficiently promote metastatic colonization of breast cancer (Korpal *et al.*, 2011), which may be due to the attenuated TGF-β signaling. Therefore, our study, together with those findings, provides novel insight into how reduced TGF-β signaling can drive metastatic tumor progression by attenuating OIS, SLGA, or other cues.

p21 is well known as a broad-specificity inhibitor of cyclin/CDK complexes and to induce SLGA in a p53-dependent manner when a cell is exposed to DNA-damaging agents, ionizing radiation, or oncogenes such as H-Ras-V12. p21 plays a key role in mediating TGF-β–induced cell cycle arrest in a p53-independent manner (Datto *et al.*, 1995). p21 is known to inhibit E2F activity by inhibiting CDKs and has been shown to regulate a host of gene transcription, primarily via its effect on E2F (Roninson, 2002). Ectopic expression of p21 was shown to reduce transcripts of many genes involved in mitosis, including CDC2, cyclin B, and CENPA, which are also identified in our microarray analysis, suggesting that the altered transcription of some genes shown in Table 1 might primarily be due to altered p21 expression and might have contributed to the escape from SLGA.

It is well known that inactivation of p53 is necessary for the escape from SLGA and for malignant transformation induced by DNA damage or oncogenic signals in various types of cells, including HMECs (Elenbaas *et al.*, 2001). Thus the malignant transformation by the abrogation of autocrine TGF-β signaling and H-Ras-V12 expression may also involve partial inactivation of p53. Indeed, we found that the ability of mitomycin C–induced p53 to increase p21 expression was attenuated in DNRII HMECs in comparison to the control, and p53 transcriptional activity was decreased by the abrogation of autocrine TGF-β signaling in DNRII HMECs as well. p53 has been shown to interact with Smad2 and enhance the transcriptional activity of Smad proteins in the promoter regions of some TGF-β target genes (Cordenonsi *et al.*, 2003; Takebayashi-Suzuki *et al.*, 2003). However, it is not clear whether Smad2 can also enhance the transcriptional activity of p53. In our study, since blockade of autocrine TGF-β signaling with DNRII expression or RIKI treatment did not significantly change total p53 levels without or with mitomycin C treatment, the reduced p53 binding to its target gene promoters in DNRII-expressing cells was likely due to the inhibition of p53 activity or the blockade of p53 binding to its *cis* element on its target gene promoters by chromatin remodeling. Studies have shown that Smad proteins cannot activate the transcription of Smad-responsive promoters in the absence of histones or chromatin templates in an in vitro transcription system. Smad2-mediated transcription requires the acetylation of nucleosomal histone H3 and H4 by p300 acetyl-transferase (Ross *et al.*, 2006). The study also showed that TGF-β–induced transcriptional activity required the interaction between phosphorylated Smad2 and the ATPase subunit Brg1 of the human SWI/SNF chromatin remodeling complex, BAF and PBAF. Thus TGF-β/Smad–regulated transcription involves chromatin remodeling. Because Smad-binding elements are between two p53 binding elements ~400–500 base pairs apart in the human p21 promoter (Gartel and Tyner, 1999; Seoane *et al.*, 2004), we speculate that blockade of TGF-β signaling reduces Smad proteins at the p21 promoter, resulting in altered chromatin structure and reduced access to the *cis* binding element by p53.

While this article was in preparation, an article appeared reporting that TGF-β signaling is required for oncogenic Ras-induced senescence in a p53- and p21-independent manner in HMECs that are not immortalized by exogenous hTERT (Cipriano *et al.*, 2011). In that study, it was shown that although ectopic expression of an oncogenic Ras induced p21 expression and SLGA in HMECs, the growth arrest could not be rescued by stable knockdown of p53 or p53 together with p21, indicating that p21 and p53 are not required for Ras-induced senescence. We speculate that the discrepancy between that study and our study is likely due to the expression of hTERT in our HMECs resulting in different sensitivity to Ras-induced SLGA.

In untransformed and early neoplastic epithelial cells, TGF-β can potently inhibit cell proliferation by maintaining the Rb protein in hypophosphorylated state via the stimulation of CDK inhibitors p15ink4b and p21 (Derynck, 1994; Miyazono *et al.*, 1994) and the inhibition of Cdc2/Cdk1 (Howe *et al.*, 1991; Fautsch *et al.*, 1995). TGF-β has also been shown to inhibit the expression of c-Myc (Coffey *et al.*, 1988; Mulder *et al.*, 1988; Pietenpol *et al.*, 1990), which in turn can also regulate the expression of cell cycle–related proteins and induce Rb phosphorylation (Dang, 1999). As such, the TGF-β autocrine pathway is tumor suppressive, and various components in the pathway have been shown to be mutationally inactivated during carcinogenesis (Massague, 2008). In our study, the DNRII- or RIKI-attenuated TGF-β signaling resulted in the escape of Ras-induced SLGA in immortalized HMECs, providing evidence that TGF-β suppresses tumorigenesis not only by simply inhibiting cell cycle, but also by mediating oncogene-induced senescence. Of interest, the attenuation of autocrine TGF-β signaling by DNRII not only promoted tumorigenicity of oncogenic Ras-transfected HMECs, but also increased their metastatic potential. Although the higher number of spontaneous lung metastases induced by orthotically inoculated DNRII + Ras cell in comparison to those induced by the Ras clones may be due to the higher primary tumor burden in the DNRII + Ras cell–inoculated mice, our results in the tail vein injection experiment demonstrate that the attenuation of autocrine TGF-β signaling enhanced Ras-induced metastatic potential of the hTERT-immortalized HMECs.

In summary, our results indicate that p21 appears to be a major player in mediating Ras-induce SLGA, as well as in the suppression of SLGA, when autocrine TGF-β signaling is attenuated in hTERT-immortalized HMECs. As such, the novelty of our study is twofold. First, it identifies p21 as the major mediator of Ras-induced SLGA in a TGF-β signaling–dependent manner in HMECs. Second, it establishes a series of isogenic basal-like breast cancer progression models that share many similarities with triple-negative, basal-like human breast carcinomas with respect to aberrant regulation of TGF-β and Ras signaling pathways, and clinical and pathological features.

MATERIALS AND METHODS

Ethics statement

All animal experiments were conducted following appropriate guidelines. They were approved by the ethics committee/institutional review board, Institutional Animal Care and Use Committee (Institutional Animal Care and Use Committee approval ID 99142×3411A), and monitored by the Department of Laboratory Animal Resources at the University of Texas Health Science Center at San Antonio.

Chemical

The small TGF-β RI kinase inhibitor, called LY-364947, is an ATP-competitive inhibitor of TGF-β RI kinase. The compound [3-(pyridine-2yl)-4-(4-quinonyl)]-1H pyrazole was synthesized according to the procedure described by Sawyer *et al*. (2003). The DNA-damaging agent mitomycin C is from Sigma-Aldrich (St. Louis, MO).

Cell culture

The human mammary epithelial cell line was originally obtained from Cambrex (Walkersville, MD) and cultured in mammary epithelial cell growth medium (MEGM) plus MEGM Bullet kit from Cambrex. Human untransformed mammary epithelial cell line MCF-10A was obtained from the Michigan Cancer Foundation (Detroit, MI) and cultured in DMEM-F12 supplemented with 5% horse serum, epidermal growth factor, $NaHCO_3$, hydrocortisone, insulin, fungizone, $CaCl_2$, cholera toxin, and antibiotics. The human breast cancer cell lines ZR-75, BT20, Hs578T, and MDA-MB-231 were originally obtained from the American Type Culture Collection (Manassas, VA). The human breast cancer cell line MCF-7 was originally obtained from the Michigan Cancer Foundation. The human breast cancer cell lines HCC1937 and HCC3153 were provided by author G.T. These cell lines were cultured in McCoy's 5A medium supplemented with pyruvate, vitamins, amino acids, antibiotics, and 10% fetal bovine serum, as described previously (Sun and Chen, 1997). Working cultures were maintained at 37°C in a humidified incubator with 5% CO_2.

3-(4,5-Dimethylthiazol-2-yl)-2,5-diphenyltetrazolium bromide assay

Cells were plated in a 96-well plate at 2000/well with indicated treatment. Two hours before each time point, 50 μl of 3-(4,5-dimethylthiazol-2-yl)-2,5-diphenyltetrazolium bromide (MTT; 2 mg/ml in phosphate-buffered saline [PBS]) was added into each well, and cells were incubated at 37°C for another 2 h. Dimethyl sulfoxide (100 μl) was added into each well after the medium was removed. For dissolving the precipitation, the plate was gently shaken on a shaker for 10 min. The absorbance was measured at 595 nm with a Microplate Reader (Bio Tek Instrument, Winooski, VT).

Cell transfection

HMECs were immortalized with ectopic expression of hTERT as reported (Elenbaas *et al*., 2001). Immortalized HMECs were infected with a pLPCX retrovirus vector (Clontech, Mountain View, CA) carrying a blasticidin-resistant gene to generate the control cell or with the vector containing DNRII cDNA to generate the HMEC DNRII cells. The sequence information of DNRII cDNA is as described previously (Ko *et al*., 1998). Forty-eight hours after the infection, selection of blasticidin-resistant cells was conducted for 1 wk. HMEC DNRII cells and HMEC control cells were infected with control pLXSN retrovirus vector containing a hygromycin-resistant gene and the H-Ras-V12 cDNA (provided by Peter J. Hornsby, University of Texas Health Science Center at San Antonio) to generate HMEC DNRII + Ras and HMEC control + Ras cells, respectively. Forty-eight hours after the infection, selection of hygromycin-resistant cells was conducted for 1 wk.

Western blot analysis

Western blot analysis was performed as described previously (Lei *et al*., 2002). Antibodies to P-Rb, P-Erk, P-Akt, and P-Smad2 were from Cell Signaling Technology (Danvers, MA), antibody to T-Smad2/3 was from BD Transduction Laboratories (San Jose, CA), antibody to fibronectin was from Life Technologies (Carlsbad, CA), antibody to RII was from Abcam (Cambridge, MA), and antibodies to H-Ras, p15ink4b, p21, and p53 were from Santa Cruz Biotechnology (Santa Cruz, CA).

Luciferase assay

Cells were transfected with a Smad-responsive promoter-luciferase construct (pSBE4-Luc) provided by Bert Vogelstein (Johns Hopkins Medical School, Baltimore, MD) and a β-gal expression plasmid by using Lipofectamine 2000 (Invitrogen, Carlsbad, CA). Five hours after the transfection, the cells were treated with or without TGF-β3 at 5 ng/ml for 24 h. Luciferase activity in the cell lysate was normalized with β-gal activity and is presented as relative luciferase activity (RLU) after normalizing the value with TGF-β to that without TGF-β respectively for each cell line. Data are presented as mean ± SEM of three transfections.

SA-β-gal assay

SA-β-gal assay was performed following the procedure described previously (Dimri *et al*., 1995). Accordingly, subconfluent cultures of various cells were fixed with 3% formaldehyde for 5 min and then incubated with a staining solution containing 0.5 mg of x-gal per milliliter of PBS for 3 h to overnight. Senescent cells containing SA-β-gal activity were stained with a blue color.

Isolation of Ras clones from soft agarose

To obtain the senescent HMEC control + Ras cells spontaneously escaped from Ras-induced SLGA in a semisolid medium, cells were suspended in 1 ml of 0.4% low–melting point agarose (Life Technologies) dissolved in the regular culture medium and plated on the top of a 1-ml underlayer of 0.8% agarose in the same medium in six-well culture plates. After 3–4 wk of incubation in the humidified incubator with 5% CO_2 at 37°C, the cell colonies were picked and plated into T25 flasks for culture.

TGF-β detection by sandwich enzyme-linked immunosorbent assay

The media conditioned by confluent cultures of various cell lines in six-well culture plates containing 2 ml of basic medium for 48 h were used for the measurements of total or active TGF-β1 and TGF-β2 with sandwich enzyme-linked immunosorbent assay (sELISA) kits

(Promega, Madison, WI). The assay was carried out according to the manufacturer's protocol.

Tumorigenicity and in vivo spontaneous lung metastatic study

Four-week-old female athymic nude mice (Harlan Sprague Dawley, Indianapolis, IN) were used for in vivo animal experiments. The animals were housed under specific pathogen-free conditions. All animal protocols were approved and monitored by the institutional animal care and use committee. EGFP in the retroviral vector pLXSN (Clontech) was stably transfected into the HMECs after the introduction of DNRII and Ras according to the manufacturer's protocol. EGFP-expressing HMEC DNRII + Ras (4×10^6 cells/site), Ras cl.4 (10×10^6 cells/site), Ras cl.1 (10×10^6 cells/site), and HMEC DNRII cells (10×10^6 cells/site) were separately inoculated into both inguinal mammary fat pads of nude mice. The suspended cells were mixed with Matrigel at 1:1 ratio before injection. Orthotopic injection of 5×10^6 cells of various Ras clones did not yield any tumors in our initial study. Therefore we injected 10×10^6 cells for Ras clones and 4×10^6 cells for DNRII + Ras cells in our subsequent studies. The tumor sizes were measured with a caliper in two dimensions. Tumor volumes (V) were calculated with the equation $V = (L \times W^2) \times 0.5$, where L is length and W is width. Animals were killed 4 or 6 wk after tumor cell inoculation. The green metastatic cancer cell colonies of different sizes were visually observed, counted, and measured in the whole lungs using a Nikon (Melville, NY) fluorescence microscope (TE-200) with a 40× objective (200× magnification). All tumor specimens were embedded in paraffin and stained with human ER-α antibody (Lab Vision, Fremont, CA) or hematoxylene and eosin for histological analysis.

Experimental in vivo lung metastasis assay

A tail vein injection model for experimental lung metastasis was used for this study. EGFP-expressing HMEC DNRII + Ras or Ras cl.4 cells were harvested from subconfluent exponentially growing cultures. The cells (0.2×10^6 cells in 200 µl of serum-free medium) were injected into the tail vein of 5-wk-old female nude mice using a mouse restrainer and a 27G needle attached to a 1-ml syringe. At the termination of experiment after 10 wk, whole lungs were excised, and EGFP-expressing metastatic cancer cell colonies were visually observed and counted under the Nikon fluorescence microscope, followed by fixation in 10% buffered formalin. All lung specimens were embedded in paraffin and stained with hematoxylene and eosin for histological analysis.

Gene microarray

Total RNA was extracted from near-confluent HMEC control, HMEC DNRII, DNRII + Ras, Ras-SLGA, and Ras cl.4 cells. Standard procedures for total RNA isolation, labeling, and hybridization using GeneChipH Human Genome U133 Plus 2.0 Array (Affymetrix, Santa Clara, CA) and microarray CEL data analysis are followed as described previously (Moore *et al*., 2005; Mukhopadhyay *et al*., 2011). Briefly, the RNA was purified using a RiboPure Kit (Ambion, Austin, TX) according to the manufacturer's protocol. The quality and quantity of RNA were ensured using the Bioanalyzer (Agilent, Santa Clara, CA) and NanoDrop (Thermo Scientific, Waltham, MA), respectively. For RNA labeling, total RNA (5 µg) was used in conjunction with the Affymetrix-recommended protocol with One-Cycle Target Labeling and Control Reagents per labeling. After the hybridization cocktail containing the fragmented and labeled cDNAs was hybridized to the chips, the chips were washed and stained by the Affymetrix Fluidics Station using the standard format and protocols from Affymetrix. The probe arrays were stained with streptavidin phycoerythrin solution (Molecular Probes, Carlsbad, CA) and enhanced by using an antibody solution containing 0.5 mg/ml biotinylated anti-streptavidin (Vector Laboratories, Burlingame, CA). The probe arrays were scanned using an Affymetrix Gene Chip Scanner 3000. Gene expression intensities were calculated using the Gene Chip Operating software 1.2 (Affymetrix). Duplicate labeling and hybridization were applied to each cell line. A GC-corrected robust multichip average model was used to correct for background, optical distortion, and nonspecific binding. Probe sets with very low expression levels in most of the arrays and little differential variation across arrays were removed by nonspecific filtering. Patterns of significantly up- and down-regulated genes across arrays were visualized by an empirical Bayes-modified hierarchical clustering. Clustering was conducted after the standardization of expression values. All analyses were performed using procedures in the R/Bioconductor suite (Gentleman *et al*., 2005). All microarray data are Minimum Information About a Microarray Experiment compliant.

Real-time PCR

Real-time PCR was performed using Brilliant SYBR Green QPCR Master Mix (Stratagene, La Jolla, CA) in the ABI 7900HT (Foster City, CA) according to the manufacturer's instruction. The relative transcript level for each transcript was calculated according the equation $2^{-ctX}/2^{-ctN}$, where X is the target gene and N is β-actin.

Chromatin immunoprecipitation and real-time qPCR

ChIP was performed essentially as previously described (Frank *et al*., 2001). Chromatin was cross-linked by addition of formaldehyde directly to cell culture medium to a final concentration of 1% at room temperature for 10 min. Fixation was stopped by the addition of glycine to a final concentration of 0.125 M, followed by next incubation for 5 min. Plates were washed twice with PBS and harvested in a SDS buffer containing protease inhibitors. Cells were pelleted and then resuspended in ice-cold IP buffer for sonication. Chromatin in a 15-ml tube was sonicated to an average length of 300–1000 base pairs. Sonication was confirmed by agarose gel electrophoresis. Triplicate protein in IP buffer was precleared with salmon sperm/protein A agarose beads. An aliquot was saved as input control. p53 primary antibody (Santa Cruz Biotechnology) was added overnight at 4°C. The next day, salmon sperm/protein A agarose was added and then incubated, followed by washes. Input controls and washed immune complex pellets were incubated overnight to elute immune complexes and to reverse the cross-links. A proteinase K solution was added to elute chromatin, followed by phenol/chloroform/isoamyl alcohol extraction and ethanol precipitation. Pelleted chromatin was resuspended in H_2O. Real-time PCR was performed in a 384-well plate on an ABI Prism 7900HT (Applied Biosystems, Foster City, CA) with SYBR Green PCR Master Mix containing appropriate primers. Percentage total promoter occupancy was calculated as previously described (Frank *et al*., 2001).

Knockdown of p21

p21 shRNA was constructed by inserting 5′-GAT CCC Cct tcg act ttg tca ccg agT TCA AGA GAc tcg gtg aca aag tcg aag TTT TTG GAA A-3′ between the *Bgl*II and *Hin*dIII sites of the pSUPER Retrovirus-puro vector (OriGene, Rockville, MD). The control vector, pSUPER Retrovirus-puro, only contains the puromycin-resistant gene and no p21 shRNA. The p21 shRNA and control plasmids were transfected into PA317 cells by using FuGENE 6 transfection reagent (Roche, Indianapolis, IN), following the manufacturer's protocol. Forty-eight hours after transfection, viral supernatants were

harvested for infection with polybrene (Sigma-Aldrich) into HMEC cells. Forty-eight hours after infection, positive cells were selected with puromycin for 1 wk.

Statistical analysis

For the comparison between two means, two-tailed Student's *t* tests are performed. A Mann–Whitney *U* test is used for comparisons made between any two groups of data within an experiment that are not normally distributed. In the experiments in which comparisons are made between more than two treatment groups, one-way analysis of variance (ANOVA) is used, followed by post hoc testing using the Tukey–Kramer multiple comparison test. For the comparison of metastasis incidence, a Fisher exact test is performed. In all cases, data are accepted as statistically significant given a probability value of ≤0.05. All statistical analysis was performed with Prism 3.03 software (GraphPad, La Jolla, CA).

ACKNOWLEDGMENTS

This work was supported in part by National Institutes of Health Grants R01CA75253 and R01CA79683 and the Cancer Therapy and Research Center at the University of Texas Health Science Center at San Antonio (UTHSCSA) through National Cancer Institute Cancer Center Support Grant 2 P30 CA054174-17. We thank Andrew Hinck (UTHSCSA) for the recombinant TGF-β3, Peter J. Hornsby (UTHSCSA) for the H-Ras-V12 expression plasmid, Xinhua Feng (Baylor College of Medicine, Houston, TX) for the p21 promoter-Luc report plasmid, Gokul Das (Roswell Park Cancer Institute, Buffalo, NY) for the PCNA promoter-Luc report plasmid, and Bert Vogelstein (Johns Hopkins Medical School) for the pSBE4-Luc plasmid. We also thank James Jackson (MD Anderson Cancer Center, Houston, TX) for technical assistance with the chromatin immunoprecipitation assay.

REFERENCES

Adorno M *et al.* (2009). A mutant-p53/Smad complex opposes p63 to empower TGFbeta-induced metastasis. Cell 137, 87–98.

Bandyopadhyay A, Zhu Y, Cibull ML, Bao L, Chen C, Sun L (1999). A soluble transforming growth factor beta type III receptor suppresses tumorigenicity and metastasis of human breast cancer MDA-MB-231 cells. Cancer Res 59, 5041–5046.

Bartkova J *et al.* (2005). DNA damage response as a candidate anti-cancer barrier in early human tumorigenesis. Nature 434, 864–870.

Bierie B, Moses HL (2006). TGF-beta and cancer. Cytokine Growth Factor Rev 17, 29–40.

Bild AH *et al.* (2006). Oncogenic pathway signatures in human cancers as a guide to targeted therapies. Nature 439, 353–357.

Bottinger EP, Jakubczak JL, Haines DC, Bagnall K, Wakefield LM (1997a). Transgenic mice overexpressing a dominant-negative mutant type II transforming growth factor beta receptor show enhanced tumorigenesis in the mammary gland and lung in response to the carcinogen 7,12-dimethylbenz-[a]-anthracene. Cancer Res 57, 5564–5570.

Bottinger EP, Jakubczak JL, Roberts IS, Mumy M, Hemmati P, Bagnall K, Merlino G, Wakefield LM (1997b). Expression of a dominant-negative mutant TGF-beta type II receptor in transgenic mice reveals essential roles for TGF-beta in regulation of growth and differentiation in the exocrine pancreas. EMBO J 16, 2621–2633.

Braig M, Lee S, Loddenkemper C, Rudolph C, Peters AH, Schlegelberger B, Stein H, Dorken B, Jenuwein T, Schmitt CA (2005). Oncogene-induced senescence as an initial barrier in lymphoma development. Nature 436, 660–665.

Carey LA *et al.* (2006). Race, breast cancer subtypes, and survival in the Carolina Breast Cancer Study. JAMA 295, 2492–2502.

Chen Z *et al.* (2005). Crucial role of p53-dependent cellular senescence in suppression of Pten-deficient tumorigenesis. Nature 436, 725–730.

Cipriano R, Kan CE, Graham J, Danielpour D, Stampfer M, Jackson MW (2011). TGF-beta signaling engages an ATM-CHK2-p53-independent RAS-induced senescence and prevents malignant transformation in human mammary epithelial cells. Proc Natl Acad Sci USA 108, 8668–8673.

Coffey RJ Jr, Bascom CC, Sipes NJ, Graves-Deal R, Weissman BE, Moses HL (1988). Selective inhibition of growth-related gene expression in murine keratinocytes by transforming growth factor beta. Mol Cell Biol 8, 3088–3093.

Collado M *et al.* (2005). Tumour biology: senescence in premalignant tumours. Nature 436, 642.

Cordenonsi M, Dupont S, Maretto S, Insinga A, Imbriano C, Piccolo S (2003). Links between tumor suppressors: p53 is required for TGF-beta gene responses by cooperating with Smads. Cell 113, 301–314.

Dang CV (1999). c-Myc target genes involved in cell growth, apoptosis, and metabolism. Mol Cell Biol 19, 1–11.

Datto MB, Li Y, Panus JF, Howe DJ, Xiong Y, Wang XF (1995). Transforming growth factor beta induces the cyclin-dependent kinase inhibitor p21 through a p53-independent mechanism. Proc Natl Acad Sci USA 92, 5545–5549.

de Jong JS, van Diest PJ, van der Valk P, Baak JP (1998). Expression of growth factors, growth inhibiting factors, and their receptors in invasive breast cancer. I: An inventory in search of autocrine and paracrine loops. J Pathol 184, 44–52.

Derynck R (1994). TGF-beta-receptor-mediated signaling. Trends Biochem Sci 19, 548–553.

Dimri GP *et al.* (1995). A biomarker that identifies senescent human cells in culture and in aging skin in vivo. Proc Natl Acad Sci USA 92, 9363–9367.

Ding Z *et al.* (2011). SMAD4-dependent barrier constrains prostate cancer growth and metastatic progression. Nature 470, 269–273.

Elenbaas B, Spirio L, Koerner F, Fleming MD, Zimonjic DB, Donaher JL, Popescu NC, Hahn WC, Weinberg RA (2001). Human breast cancer cells generated by oncogenic transformation of primary mammary epithelial cells. Genes Dev 15, 50–65.

Fautsch MP, Eblen ST, Anders RA, Burnette RJ, Leof EB (1995). Differential regulation of p34cdc2 and p33cdk2 by transforming growth factor-beta 1 in murine mammary epithelial cells. J Cell Biochem 58, 517–526.

Frank SR, Schroeder M, Fernandez P, Taubert S, Amati B (2001). Binding of c-Myc to chromatin mediates mitogen-induced acetylation of histone H4 and gene activation. Genes Dev 15, 2069–2082.

Gartel AL, Tyner AL (1999). Transcriptional regulation of the p21((WAF1/CIP1)) gene. Exp Cell Res 246, 280–289.

Gentleman R, Carey V, Huber W, Irizarry R, Dudoit S (2005). Bioinformatics and Computational Biology Solutions Using R and Bioconductor, New York: Springer-Verlag.

Gobbi H, Dupont WD, Simpson JF, Plummer WD Jr, Schuyler PA, Olson SJ, Arteaga CL, Page DL (1999). Transforming growth factor-beta and breast cancer risk in women with mammary epithelial hyperplasia. J Natl Cancer Inst 91, 2096–2101.

Howe PH, Draetta G, Leof EB (1991). Transforming growth factor beta 1 inhibition of p34cdc2 phosphorylation and histone H1 kinase activity is associated with G1/S-phase growth arrest. Mol Cell Biol 11, 1185–1194.

Jemal A, Siegel R, Xu J, Ward E (2010). Cancer statistics, 2010. CA Cancer J Clin 60, 277–300.

Ko Y, Koli KM, Banerji SS, Li W, Zborowska E, Willson JK, Brattain MG, Arteaga CL (1998). A kinase-defective transforming growth factor-beta receptor type II is a dominant-negative regulator for human breast carcinoma MCF-7 cells. Int J Oncol 12, 87–94.

Korpal M *et al.* (2011). Direct targeting of Sec23a by miR-200s influences cancer cell secretome and promotes metastatic colonization. Nature Med 17, 1101–1108.

Lei X, Bandyopadhyay A, Le T, Sun L (2002). Autocrine TGFbeta supports growth and survival of human breast cancer MDA-MB-231 cells. Oncogene 21, 7514–7523.

Livasy CA, Karaca G, Nanda R, Tretiakova MS, Olopade OI, Moore DT, Perou CM (2006). Phenotypic evaluation of the basal-like subtype of invasive breast carcinoma. Mod Pathol 19, 264–271.

Lynch MA *et al.* (2001). Responsiveness to transforming growth factor-beta (TGF-beta)-mediated growth inhibition is a function of membrane-bound TGF-beta type II receptor in human breast cancer cells. Gene Expr 9, 157–171.

Massague J (2008). TGFbeta in cancer. Cell 134, 215–230.

Michaloglou C, Vredeveld LC, Soengas MS, Denoyelle C, Kuilman T, van der Horst CM, Majoor DM, Shay JW, Mooi WJ, Peeper DS (2005). BRAFE600-associated senescence-like cell cycle arrest of human naevi. Nature 436, 720–724.

Minn AJ, Gupta GP, Siegel PM, Bos PD, Shu W, Giri DD, Viale A, Olshen AB, Gerald WL, Massague J (2005). Genes that mediate breast cancer metastasis to lung. Nature 436, 518–524.

Missero C, Di Cunto F, Kiyokawa H, Koff A, Dotto GP (1996). The absence of p21Cip1/WAF1 alters keratinocyte growth and differentiation and promotes ras-tumor progression. Genes Dev 10, 3065–3075.
Miyazono K, ten Dijke P, Yamashita H, Heldin CH (1994). Signal transduction via serine/threonine kinase receptors. Semin Cell Biol 5, 389–398.
Moore DF *et al.* (2005). Using peripheral blood mononuclear cells to determine a gene expression profile of acute ischemic stroke: a pilot investigation. Circulation 111, 212–221.
Mukhopadhyay KD, Bandyopadhyay A, Chang TT, Elkahloun AG, Cornell JE, Yang J, Goins BA, Yeh IT, Sun LZ (2011). Isolation and characterization of a metastatic hybrid cell line generated by ER negative and ER positive breast cancer cells in mouse bone marrow. PloS One 6, e20473.
Mulder KM, Levine AE, Hernandez X, McKnight MK, Brattain DE, Brattain MG (1988). Modulation of c-myc by transforming growth factor-beta in human colon carcinoma cells. Biochem Biophys Res Commun 150, 711–716.
Pantoja C, Serrano M (1999). Murine fibroblasts lacking p21 undergo senescence and are resistant to transformation by oncogenic Ras. Oncogene 18, 4974–4982.
Perou CM *et al.* (2000). Molecular portraits of human breast tumours. Nature 406, 747–752.
Pietenpol JA, Stein RW, Moran E, Yaciuk P, Schlegel R, Lyons RM, Pittelkow MR, Munger K, Howley PM, Moses HL (1990). TGF-beta 1 inhibition of c-myc transcription and growth in keratinocytes is abrogated by viral transforming proteins with pRB binding domains. Cell 61, 777–785.
Pouliot F, Labrie C (1999). Expression profile of agonistic Smads in human breast cancer cells: absence of regulation by estrogens. Int J Cancer 81, 98–103.
Roberts AB, Wakefield LM (2003). The two faces of transforming growth factor beta in carcinogenesis. Proc Natl Acad Sci USA 100, 8621–8623.
Rocco JW, Sidransky D (2001). p16(MTS-1/CDKN2/INK4a) in cancer progression. Exp Cell Res 264, 42–55.
Rodriguez-Pinilla SM, Sarrio D, Honrado E, Hardisson D, Calero F, Benitez J, Palacios J (2006). Prognostic significance of basal-like phenotype and fascin expression in node-negative invasive breast carcinomas. Clin Cancer Res 12, 1533–1539.
Roninson IB (2002). Oncogenic functions of tumour suppressor p21(Waf1/Cip1/Sdi1): association with cell senescence and tumour-promoting activities of stromal fibroblasts. Cancer Lett 179, 1–14.
Ross DT, Perou CM (2001). A comparison of gene expression signatures from breast tumors and breast tissue derived cell lines. Dis Markers 17, 99–109.
Ross S, Cheung E, Petrakis TG, Howell M, Kraus WL, Hill CS (2006). Smads orchestrate specific histone modifications and chromatin remodeling to activate transcription. EMBO J 25, 4490–4502.
Sawyer JS *et al.* (2003). Synthesis and activity of new aryl- and heteroaryl-substituted pyrazole inhibitors of the transforming growth factor-beta type I receptor kinase domain. J Med Chem 46, 3953–3956.
Seoane J, Le HV, Shen L, Anderson SA, Massague J (2004). Integration of Smad and forkhead pathways in the control of neuroepithelial and glioblastoma cell proliferation. Cell 117, 211–223.
Serrano M, Lin AW, McCurrach ME, Beach D, Lowe SW (1997). Oncogenic ras provokes premature cell senescence associated with accumulation of p53 and p16INK4a. Cell 88, 593–602.
Sorlie T *et al.* (2001). Gene expression patterns of breast carcinomas distinguish tumor subclasses with clinical implications. Proc Natl Acad Sci USA 98, 10869–10874.
Stuelten CH, Buck MB, Dippon J, Roberts AB, Fritz P, Knabbe C (2006). Smad4-expression is decreased in breast cancer tissues: a retrospective study. BMC Cancer 6, 25.
Sun L, Chen C (1997). Expression of transforming growth factor beta type III receptor suppresses tumorigenicity of human breast cancer MDA-MB-231 cells. J Biol Chem 272, 25367–25372.
Takebayashi-Suzuki K, Funami J, Tokumori D, Saito A, Watabe T, Miyazono K, Kanda A, Suzuki A (2003). Interplay between the tumor suppressor p53 and TGF beta signaling shapes embryonic body axes in *Xenopus*. Development 130, 3929–3939.
Tremain R, Marko M, Kinnimulki V, Ueno H, Bottinger E, Glick A (2000). Defects in TGF-beta signaling overcome senescence of mouse keratinocytes expressing v-Ha-ras. Oncogene 19, 1698–1709.
Troester MA, Hoadley KA, Sorlie T, Herbert BS, Borresen-Dale AL, Lonning PE, Shay JW, Kaufmann WK, Perou CM (2004). Cell-type-specific responses to chemotherapeutics in breast cancer. Cancer Res 64, 4218–4226.
van't Veer LJ *et al.* (2002). Gene expression profiling predicts clinical outcome of breast cancer. Nature 415, 530–536.
Vijayachandra K, Lee J, Glick AB (2003). Smad3 regulates senescence and malignant conversion in a mouse multistage skin carcinogenesis model. Cancer Res 63, 3447–3452.
Wang XJ, Greenhalgh DA, Bickenbach JR, Jiang A, Bundman DS, Krieg T, Derynck R, Roop DR (1997). Expression of a dominant-negative type II transforming growth factor beta (TGF-beta) receptor in the epidermis of transgenic mice blocks TGF-beta-mediated growth inhibition. Proc Natl Acad Sci USA 94, 2386–2391.
Wang Y *et al.* (2005). Gene-expression profiles to predict distant metastasis of lymph-node-negative primary breast cancer. Lancet 365, 671–679.